Synthesis of silver nanoparticles by chemical reduction method and their antibacterial activity

Maribel G. Guzmán, Jean Dille, Stephan Godet

Abstract—Silver nanoparticles were prepared by chemical reduction method. Silver nitrate was taken as the metal precursor and hydrazine hydrate as a reducing agent. The formation of the silver nanoparticles was monitored using UV-Vis absorption spectroscopy. The UV-Vis spectroscopy revealed the formation of silver nanopartícles by exhibing the typical surface plasmon absorption maxima at 418-420 nm from the UV–Vis spectrum. Comparison of theoretical (*Mie* light scattering theory) and experimental results showed that diameter of silver nanoparticles in colloidal solution is about 60 nm. We have used energy-dispersive spectroscopy (EDX), X-ray diffraction (XRD), transmission electron microscopy (TEM) and, UV–Vis spectroscopy to characterize the nanoparticles obtained. The energy-dispersive spectroscopy (EDX) of the nanoparticles dispersion confirmed the presence of elemental silver signal no peaks of other impurity were detected. The average size and morphology of silver nanoparticles were determined by transmission electron microscopy (TEM). TEM photographs indicate that the nanopowders consist of well dispersed agglomerates of grains with a narrow size distribution (40 and 60 nm), whereas the radius of the individual particles are between 10 and 20 nm. The synthesized nanoparticles have been structurally characterized by X-ray diffraction and transmission high-energy electron diffraction (HEED). The peaks in the XRD pattern are in good agreement with the standard values of the face-centered-cubic form of metallic silver (ICCD-JCPDS card no. 4-0787) and no peaks of other impurity crystalline phases were detected. Additionally, the antibacterial activity of the nanopartículas dispersion was measured by Kirby-Bauer method. The nanoparticles of silver showed high antimicrobial and bactericidal activity against gram positive bacteria such as *Escherichia Coli*, *Pseudimonas aureginosa* and *staphylococcus aureus* which is a highly methicillin resistant strain.

Keywords— Silver nanoparticles, surface plasmon, UV-Vis absorption Spectrum, chemicals reduction.

I. INTRODUCTION

In recent years noble metal nanoparticles have been the subjects of focused researches due to their unique electronic, optical, mechanical, magnetic and chemical properties that are significantly different from those of bulk materials [1]. These special and unique properties could be attributed to their small

M. Guzman works at Engineering Department of Pontificia Universidad Catolica del Peru, Av. Universitaria 1801, Lima-32, PERU. (corresponding author to provide phone: ++(511)-626.2000 (extension 5000); fax: ++(511)-626.2852; e-mail: mguzman@pucp.edu.pe).

J. Dille works at Matters and materials Section of Université Libre de Bruxelles, Belgium, 50 Avenue Roosevelt CP 194/03, B-1050 Brussels, Belgium (e-mail: jdille@ulb.ac.be).

sizes and large specific surface area. For these reasons metallic nanoparticles have found uses in many applications in deferent fields as catalysis, electronics, and photonics. A variety of preparation routes have been reported for the preparation of metallic nanoparticles [2,3]; notable examples include, reverse micelles process [4,5], salt reduction [6], microwave dielectric heating reduction [7], ultrasonic irradiation [8], radiolysis [9,10], solvothermal synthesis [11], electrochemical synthesis [12,13], etc. In recent years nanoparticles of silver have been found to exhibit interesting antibacterial activities [14,15].

Presently, the investigation of this phenomenon has regained importance due to the increase of bacterial resistance to antibiotics, caused by their overuse. Recently, silver nanoparticles exhibiting antimicrobial activity have been synthesized [16]. Antibacterial activity of the silver-containing materials can be used, for example, in medicine to reduce infections as well as to prevent bacteria colonization on prostheses [17], catheters [18,19], vascular grafts [20], dental materials [5], stainless steel materials [21] and human skin [5,22].

The use of silver nanoparticles as antibacterial agent is relatively new. Because of their high reactivity due to the large surface to volume ratio, nanoparticles play a crucial role in inhibiting bacterial growth in aqueous and solid media. Silver-containing materials can be employed to eliminate microorganisms on textile fabrics [12,23] or they can be used for water treatment [24]. Contrary to bactericide effects of ionic silver, the antimicrobial activity of colloid silver particles are influenced by the dimensions of the particles the smaller the particles, the greater antimicrobial effect [14]. Therefore, in developing routes of synthesis, an emphasis was made to control the size of silver nanoparticles. Silver nanoparticles have been produced using different methods: electrochemical method [25-27], thermal decomposition [28], laser ablation [29], microwave irradiation [30] and sonochemical synthesis [31]. The simplest and the most commonly used bulk-solution synthetic method for metal nanoparticles is the chemical reduction of metal salts [32,33]. In fact, production of nanosized metal silver particles with different morphologies and sizes [34] using chemical reduction of silver salts has been reported [35]. This synthetic method involves reduction of an ionic salt in an appropriate medium in the presence of surfactant using various reducing agents [36].

The dispersions of silver nanoparticles display intense colors due to the plasmon resonance absorption. The surface of a metal is like a plasma, having free electrons in the conduction band and positively charged nuclei. Surface

Plasmon resonance is a collective excitation of the electrons in the conduction band; near the surface of the nanoparticles. Electrons are limited to specific vibrations modes by the particle's size and shape. Therefore, metallic nanoparticles have characteristic optical absorption spectrums in the UV-Vis region [37].

Antimicrobial susceptibility testing methods are divided into types based on the principle applied in each system. They include: Diffusion (*Kirby-Bauer* and *Stokes*), Dilution (Minimum Inhibitory Concentration) and Diffusion & Dilution (E-Test method). Antimicrobial susceptibility testing in the clinical laboratory is most often performed using the disc diffusion method. The Kirby-Bauer and Stokes' methods are usually used for antimicrobial susceptibility testing, with the Kirby-Bauer method being recommended by the National Committee for Clinical Laboratory Standards (NCCLS) (NCCLS, 03). The Kirby-Bauer method was originally standardized by Bauer et al. (the so called Kirby-Bauer method). This method is well documented and standard zones of inhibition have been determined for susceptible and resistant values [38,39]. The antibacterial characteristics of silver nanoparticles produced have been demonstrating by directly exposing bacteria to colloid silver particles solution [40].

In the present work on the preparation of nanosized silver nanoparticles from aqueous solution of silver nitrate, we employed as reductant a mixture of hydrazine hydrate and citrate of sodium; sodium dodecyl sulphate was employed as a stabilizer.

II. EXPERIMENTAL

A. Material

Silver nitrate ($AgNO_3$), Hydrazine hydrate, Citrate of sodium and Sodium Dodecyl Sulphate (SDS) were purchase from Merck Peruana. All chemicals were used as received. Double-distilled deionised water was used.

B. Characterization techniques

Ultraviolet-visible Spectroscopy (UV-Vis) was performed in a Perkin-Elmer Lambda 2 Spectrophotometer. The studies of size, morphology and composition of the nanoparticles were performed by means of transmission electron microscopy (TEM), energy dispersive X-ray Analysis (EDX) and high energy electron diffraction (HEED) using Phillips CM20-Ultra Twin microscope operating at 200 kV. Histograms of size distribution were calculated from the TEM images by measuring the diameters of at least 50 particles. Samples for TEM studies were prepared by placing drops of the silver nanoparticles solutions on carbon-coated TEM grids.

C. Preparation of silver nanoparticles

For the preparation of silver nanoparticles two stabilizing agents, Sodium Dodecyl Sulphate (SDS) and Citrate of sodium were used. For the synthesis of silver nanoparticles, silver nitrate solution (from 1,0 mM to 6,0 mM) and 8% (w/w)

Sodium Dodecyl Sulphate (SDS) were used as a metal salt precursor and a stabilizing agent, respectively. Hydrazine hydrate solution with a concentrate ranging from 2,0 mM to 12 mM and Citrate of sodium solution (1,0 mM to 2,0 mM) were used as a reducing agents. Citrate of sodium was also used as stabilizing agent at room temperature. The transparent colourless solution was converted to the characteristic pale yellow and pale red colour, when citrate of sodium was used as stabilizing agent. The occurrence of colour was indicated the formation of silver nanoparticles. The silver nanoparticles were purified by centrifugation. To remove excess silver ions, the silver colloids were washed at least three times with deionized water under nitrogen stream. A dried powder of the nanosize silver was obtained by freeze-drying. To carry out all characterization methods and interaction of the silver nanoparticles with bacteria, the silver nanoparticle powder in the freeze-drying cuvette was resuspended in deionized water; the suspension was homogenized with a Fisher Bioblock Scientific ultrasonic cleaning container.

D. Antibacterial assay:

The antimicrobial susceptibility of silver nanoparticles was evaluated using the disc diffusion or Kirby-Bauer method [15]. Zones of inhibition were measured after 24 hr of incubation at 35C. The comparative stability of discs containing *oxacillin* and *ciprofloxacin* was made. The standard dilution micromethod, determining the minimum inhibitory concentration (MIC) leading to inhibition of bacterial growth is under way.

III. RESULTS AND DISCUSSIONS

Silver nanoparticles were synthesized according to the method described in the previous section, the colloidal solution turned pale brown, pale yellow and pale red indicating that the silver nanoparticles were formed. Figure 1 shows the photographs of samples obtained at different conditions. The colourless Ag^+ solution containing SDS turned pale yellow-brown in addition of hydrazine solution (Fig. 1A) and in the case of adding citrate of sodium the colour changed to pale red (Fig 1C). In the case that we do not use SDS the uncolored Ag^+ solution turned pale yellow in addition of hydrazine and citrate of sodium solution at different concentrations (Fig. 1B).

UV-visible spectroscopy is one of the most widely used techniques for structural characterization of silver nanoparticles. The absorption spectrum (Fig. 2) of the pale yellow-brown silver colloids prepared by hydrazine reduction showed a surface Plasmon absorption band with a maximum of 418 nm indicating the presence of spherical or roughly spherical Ag nanoparticles, and TEM imaging confirmed this (Fig. 3). This image show agglomerates of small grains and some dispersed nanoparticles. The particle size histograms of silver particles (right-hand illustration in Figure 3) show that the particles range in size from 8 to 50 nm with mean diameter 24 nm.
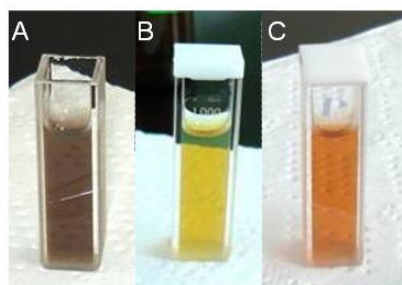
Fig.1.- Photographs of pale brown, pale yellow and pale red silver nanoparticles obtained. Ag particles prepared using hydrazine hydrate and SDS as reducing and stabilizing agent, respectively (A), both hydrazine hydrate and citrate of sodium as reducing agents.(B), hydrazine hydrate plus citrate of sodium as reducing and SDS as stabilizing agent respectively (C).

UV-visible spectroscopy is one of the most widely used techniques for structural characterization of silver nanoparticles. The absorption spectrum (Fig. 2) of the pale yellow-brown silver colloids prepared by hydrazine reduction showed a surface Plasmon absorption band with a maximum of 418 nm indicating the presence of spherical or roughly spherical Ag nanoparticles, and TEM imaging confirmed this (Fig. 3). This image show agglomerates of small grains and some dispersed nanoparticles. The particle size histograms of silver particles (right-hand illustration in Figure 3) show that the particles range in size from 8 to 50 nm with mean diameter 24 nm.
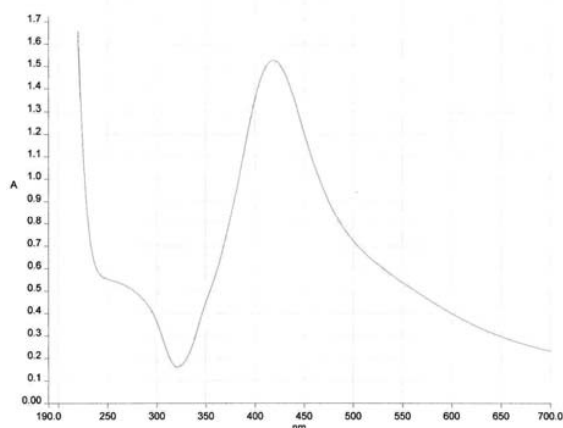
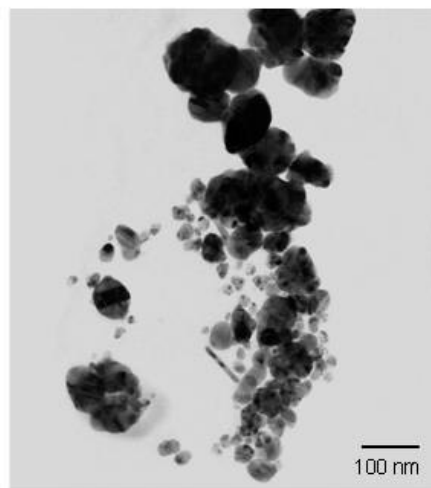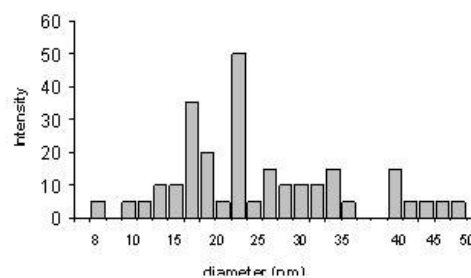Fig. 2.-UV–Vis absorption spectrum of silver nanoparticles obtained.

Fig. 3.- TEM image of spherical silver nanoparticles and its particle size distributions. Ag particles prepared from 1.1 mM $AgNO_3$ solution.

The elemental analysis of the silver nanoparticles was performed using the EDX on the TEM. Figure 4 shows the EDX spectrum of the spherical nanoparticles prepared with hydrazine hydrate as reducing agent. The peaks around 3.40 keV, 22 keV and 25 keV are correspond to the binding energies of Ag_L, Ag Ka_1 and Ag Ka_2, respectively, while the peaks situated at binding energies of 8.06 and 8.94 keV belong to $CuKa$ and $CuKb$, respectively. Also, a peak near 1.0 keV corresponding of carbon is observed. The carbon and the copper peaks correspond to the TEM holding grid. Throughout the scanning range of binding energies, no obvious peak belong to impurity is detected. The result indicates that the as-synthesized product is composed of high purity Ag nanoparticles. The similar EDX spectrum was obtained for each sample analyzed.
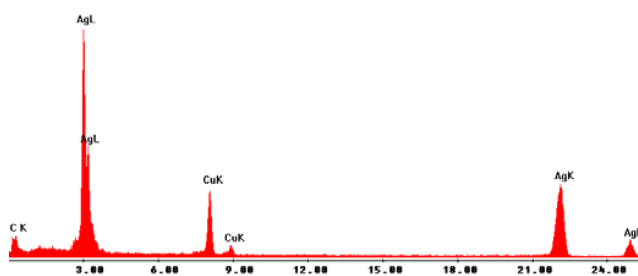
Fig.4.- Energy-dispersive spectroscopy spectrum of silver nanoparticles prepared from 1.1 mM AgNO$_3$ solution.

The UV–Vis absorption spectrum of silver nanoparticles synthesized using a mixture of hydrazine and citrate of sodium as a reducing agent and SDS as stabilizer agent is show in figure 5. UV–Vis absorption spectrum (Fig. 5) reveals the formation of silver nanoparticles by showing surface plasmon absorption maxima at 412 nm. The position and shape of the plasmon absorption depends on the particles size, shape and the dielectric constant of the surrounding medium. We can observe that surface plasmon absorption maximum initially at 418 nm (figure 3) is shifted to lower wavelength (figure 5) with addition of citrate of sodium as reducing agent. The shape of the UV–Vis absorption spectrum is also noticed. The spectrum shows a smooth shoulder near 540 nm.
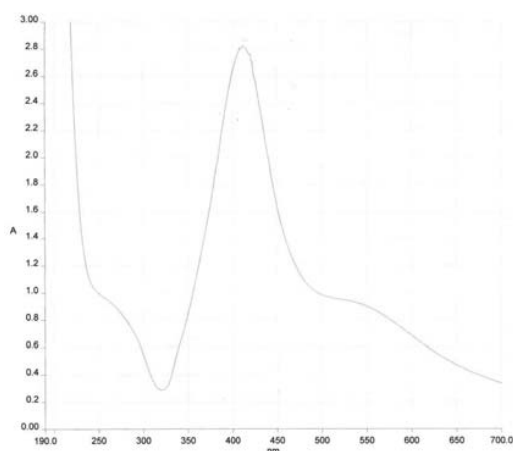

Fig. 5.- UV–Vis absorption spectrum of silver nanoparticles prepared using a mixture of hydrazine and citrate of sodium as a reducing agent.

The transmission electron microscopy (TEM) image of the silver synthesized is represented in Figure 6 and indicates well dispersed particles which are more or less spherical. The TEM illustrated in figure 6 show the presence of faceted particles. The average size of these particles is approximately 30 nm. The particle size histograms of silver particles (Figure 7) show that the particles range in size from 15 to 48 nm. In comparison with particles size obtained using only hydrazine

hydrate as reducing agent (figure 3), the mean diameter does not increase significantly. In consequence, the shifting of surface plasmon absorption maximum from 418 nm (figure 2) to 412 nm (figure 5) could be due to the difference in particle shape. The decrease of the absorbance of figure 2 in comparison figure 5 indicating a little aggregation of silver nanoparticles.

The corresponding HEED pattern of silver particles is show on the right-hand illustration in Figure 6. When the electron diffraction is carried out on a limited number of crystals one observes only some spots of diffraction distributed on concentric circles. The rings patterns with plane distances 2.36Å, 2.04Å, 1.45Å, 1.23Å and 0.94 Å are consistent with the plane families {111}, {200}, {220}, {311} and {331} of pure face-centred cubic (fcc) silver structure (JCPDS, File No. 4-0787).
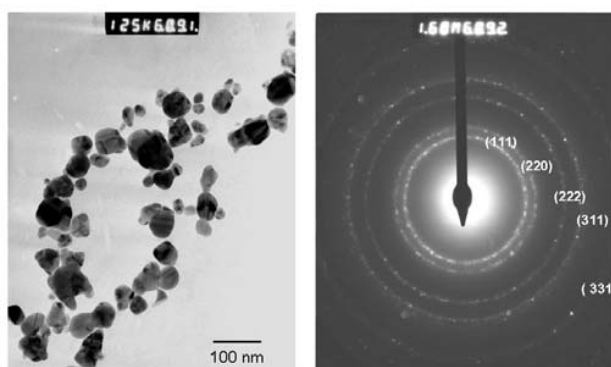

Fig. 6.- TEM and HEED images of silver nanoparticles synthesized. Metal ion concentration and citrate of sodium solution 6.0 mM and 2.0 mM, respectively.
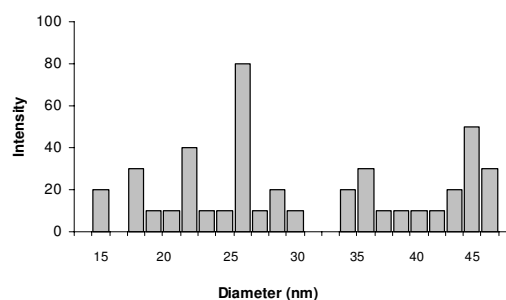

Fig. 7.- Particle size distributions of Ag nanoparticles prepared using a mixture of hydrazine and citrate of sodium as a reducing agent.

The UV-Vis absorption spectra of nanoparticles prepared using a mixture of both hydrazine hydrate and citrate of sodium at different concentrations as reducing agents were obtained (Fig. 8). The UV-Vis spectra reveals the formation of silver nanoparticles by showing surface plasmon resonance at 405 nm and 406 nm, when citrate of sodium solution with concentration of 1.0 mM and 2.0 mM were using. The spectra showed a shoulder near 520 nm. The position and shape of the plasmon absorption depends on the particles size, shape and

the dielectric constant of the surrounding medium. In this case, the shifting of surface plasmon absorption maximum from 418 nm (figure 2) to 406 nm (figure 7) is due to the difference in particles size. TEM imaging confirmed this (Fig. 9) and indicates that the nanoparticles prepared at different citrate of sodium concentrations have different shapes and similar sizes.
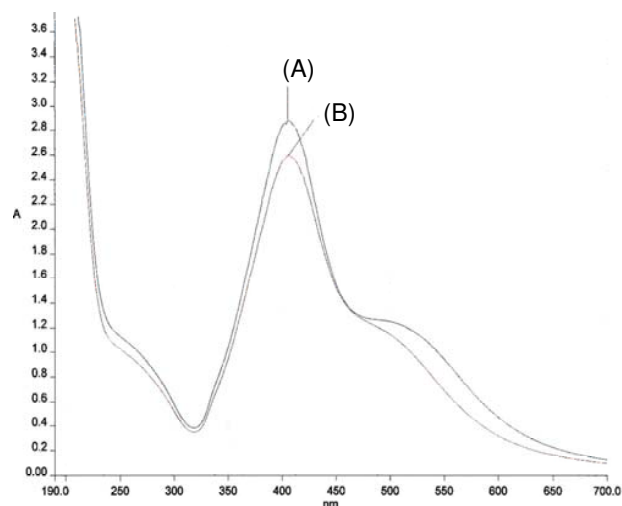

Fig. 8.- UV–Vis absorption spectrum of silver nanoparticles prepared using hydrazine hydrate (2.0 mM) and citrate of sodium solution with a concentrate ranging from 1.0 mM (A) to 2.0 mM (B).

The results by TEM indicate that the nanoparticles consist of agglomerates of small grains with mean diameters between 9 and 11 nm. However, some particles whose diameters are longer that 60 nm were formed because of aggregation during preparation of the TEM holding grid. The figure 9 (A) shows agglomerates of small grains and some dispersed nanoparticles which are more or less spherical. Fig. 9 (B) shows particles spherical and close to the square for the large ones. The particle size histograms of both samples were obtained (figure 10). The figure 10 (A) shows that the particles of silver range in size from 7 to 20 nm with mean diameter 9 nm is obtained with 1.0 mM of citrate of sodium. When a double concentration of citrate of sodium is used, the formation of silver nanoparticles with two distributions of size is formed. The figure 10 (B) shows that the particles of silver range in size from 7 to 20 nm and from 22 to 35 nm, with mean diameter 11 nm.
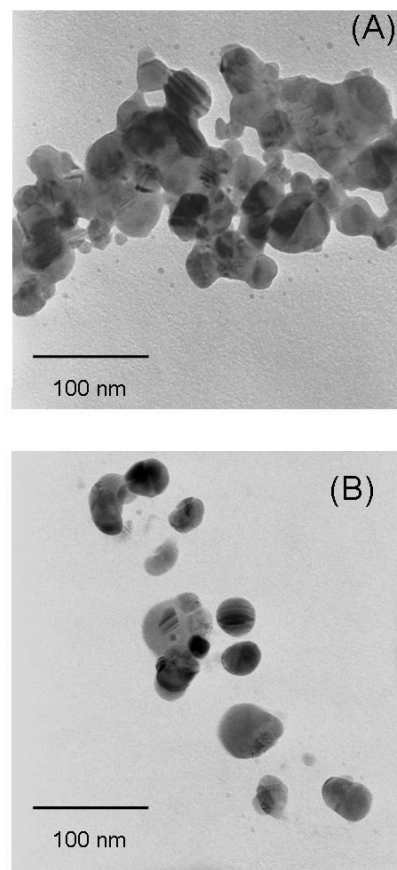

Fig. 9.- TEM image of spherical silver nanoparticles obtained at 1.0 mM (A) and 2.0 mM (B) of citrate of sodium solution.
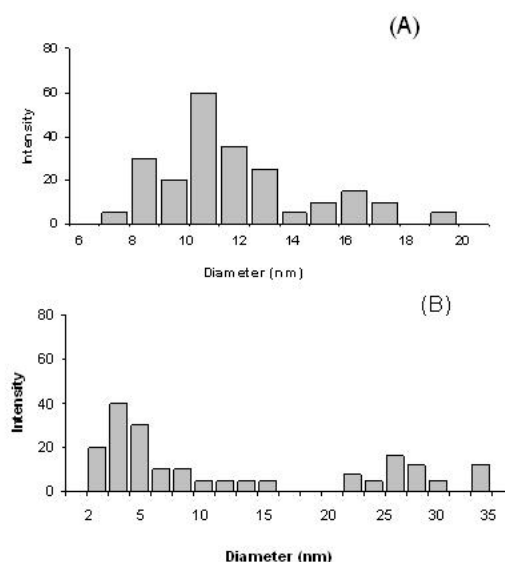

Fig.10.- Particle size distributions of Ag nanoparticles (prepared from 1.1 mM AgNO$_3$ solution) and citrate of sodium solution with a concentrate ranging from 1.0 mM (A) to 2.0 mM (B).

The particle size data obtained from TEM images analyze and UV-Vis surface plasmon absorption maxima for all samples are given in Table 1. Increase in citrate of sodium concentration show a change in particle size and λmax for silver nanoparticles obtained at lower metal ion concentration (1.1 mM). However, silver nanoparticles synthesized at higher concentration (6.0 mM) did not show any drastically change in particle size and surface plasmon absorption maxima.

TABLE I
PARTICLE SIZES AND SURFACE PLASMON ABSORPTION MAXIMA SILVER NANOPARTICLES AT DIFFERENT METAL ION AND CITRATE OF SODIUM CONCENTRATIONS.

Sample	Citrate of sodium concentration					
	0.0 mM		1.0 mM		2.0 mM	
	Particle size nm)	λmax (nm)	Particle size (nm)	λmax (nm)	Particle size (nm)	λmax (nm)
MGA[a]	24	418				
MGB[a]					30	412
MGC[b]			9	406		
MGD[b]					11	405

[a] 6.0 mM AgNO$_3$,
[b] 1.1 mM AgNO$_3$,

Finally, the antimicrobial susceptibility of silver nanoparticles synthesized was investigated. The *Kirby-Bauer* diffusion method was used as antimicrobial susceptibility testing method. Disposable plates inoculated with the tested Gram-positive and Gram-negative bacteria, including highly multiresistant strains such as methicillin-resistant *Staphylococcus aureus* at a concentration of 10^5 to 10^6 CFU/mL were used for the tests. Zones of inhibition were measured after 24 hr of incubation at 35 C. The comparative stability of discs containing *oxacillin* and *ciprofloxacin* was made.

Figure 11 shows plates to which a bacterial suspension (approximately 10^6 CFU/ml) was applied. The presence of nanoparticles at a certain level inhibited bacterial growth by more than 90%. The diameter of inhibition zones (in millimeters) around the different silver nanoparticles sols with against test strain are shown in Table 2. Decrease in particle size of silver nanoparticles show a lower susceptibility. However, it is necessary to determine the minimum inhibitory concentration de MIC of each sample.

Antimicrobial activities of the synthesized silver colloidal sols were assessed using the standard dilution micromethod, determining the minimum inhibitory concentration (MIC) leading to inhibition of bacterial growth (National Committee for Clinical Laboratory Standards. Performance standards for antimicrobial susceptibility testing. Twelfth informational supplement. NCCLS documentM100-S12. NCCLS, Wayne, Pennsylvania, 2002).
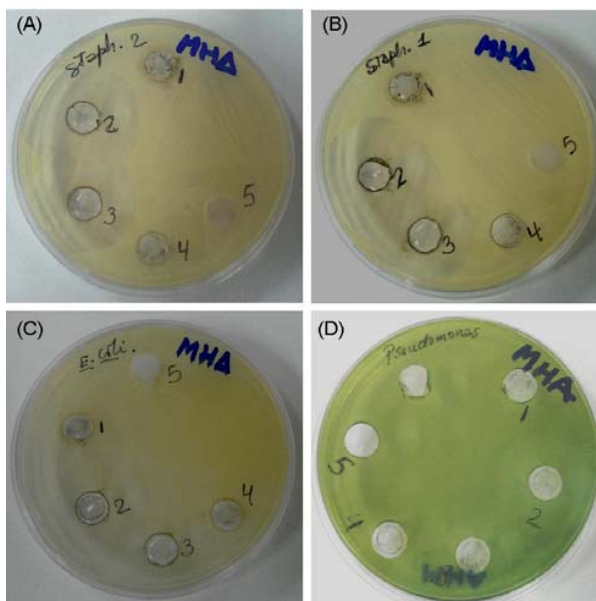

Fig. 11.- Appearances of inhibitory zones with (A) *S. aureus* (B) *methicillin-resistant S. aureus* (C) *Escherichia coli* and (D) *Pseudomonas aeruginosa* bacteria.

TABLE II
ZONE OF INHIBITION (MM) OF SILVER NANOPARTICLES SOLS PREPARED AT DIFFERENT CONDITIONS AGAINST TEST STRAINS.

bacteria	MGC ∅ = 9 nm	MGD ∅ = 11 nm	MGA ∅ = 24 nm	MGB ∅ = 30 nm
Staphylloccoccus aureus CCM 3953	12	12	35	32
Staphylococcus aureus MRSA	12	12	40	30
Escherichia coli CCM 3954	10	11	33	27
Pseudomonas aeruginosa CCM	10	11	30	20

The silver sols were diluted 2-8 times with 100 íL of Mueller-Hinton broth inoculated with the tested bacteria at a concentration of 10^5 to 10^6 CFU/mL. The minimum inhibitory concentration (MIC) was read after 24 h of incubation at 37 °C. The MIC was determined as the lowest concentration that inhibited the visible growth of the used bacterium. The silver sols were used in the form in which they had been prepared. Therefore, control bactericidal tests of solutions containing all the reaction components with the exception of silver nitrate, and reducing agents were performed. Table 3 summarizes the minimum inhibition concentrations of the tested silver particles samples against Gram-positive and Gram-negative bacteria.

TABLE III
MINIMUM INHIBITION CONCENTRATIONS OF SILVER NANOPARTICLES PREPARED VIA REDUCTION OF AgNO$_3$ BY HYDRAZINE AND CITRATE OF SODIUM REDUCING AGENTS.

	Minimum inhibition concentrations (µg/mL)			
	MGC	MGD	MGA	MGB
bacteria	$\varnothing$ = 9 nm	$\varnothing$ = 11 nm	$\varnothing$ = 24 nm	$\varnothing$ = 30 nm
Staphylloccoccus aureus CCM 3953	14.38	28.77	258.89	215.74
Staphylococcus aureus MRSA	14.38	28.77	258.89	215.74
Escherichia coli CCM 3954	14.38	28.77	258.89	215.74
Pseudomonas aeruginosa CCM 3955	14.38	28.77	6.74	215.74

Smaller silver nanoparticles synthesized using citrate of sodium shows has considerably antibacterial activity. This phenomenon is related to size of colloidal silver particles. Thus, the 9 nm and 11 nm silver particles synthesized showed the highest activity against Gram-positive and Gram-negative bacteria. The lowest antimicrobial effect against Gram-positive bacteria was observed in nanoparticles obtained with no using citrate of sodium. Nevertheless, this sample shows the highest activity against Gram-negative bacteria. The mechanism of the bactericidal effect of silver colloid particles against bacteria is not very well-known. Silver nanoparticles may attach to the surface of the cell membrane and disturb its power function such as permeability and respiration. It is reasonable to state that the binding of the particles to the bacteria depends on the surface area available for interaction. Smaller particles having the larger surface area available for interaction will give more bactericidal effect than the larger particles.

IV. CONCLUSION

In summary, silver nanoparticles with mean diameters of 9, 11, 24 and 30 nm were synthesized using hydrazine hydrate and citrate of sodium as a reducing agent. The nanoparticles were characterized by UV/Vis, EDX and TEM. UV/Vis spectra show the characteristic plasmon absorption peak for the silver nanoparticles ranging from 405 to 418 nm.

The energy-dispersive spectroscopy (EDX) of the nanoparticles dispersion confirmed the presence of elemental silver signal no peaks of other impurity were detected. High-energy electron diffraction (HEED) confirmed that formation of face-centered-cubic silver nanoparticles.

Additionally, the antibacterial activity of the nanopartículas dispersion was measured by *Kirby-Bauer* method. The results of this study clearly demonstrated that the colloidal silver nanoparticles inhibited the growth and multiplication of the tested bacteria, including highly multiresistant bacteria such as *methicillin-resistant Staphylococcus aureus*, *S. aureus*, *Escherichia coli* and *Pseudomonas aeruginosa*. Such high antibacterial activity was observed at very low total concentrations of silver below 6.74 µg/mL.

REFERENCES

[1] Mazur M. *Electrochemistry Communications* 6, (2004) 400-403.
[2] Pal A., Shah S., Devi S. *Colloids and Surfaces* A 302, (2007) 483-487.
[3] Rosemary M.J., Pradeep T. *Colloids and Surfaces* A 268, (2003) 81-84.
[4] Xie Y., Ye R., Liu H. *Colloids and Surfaces* A 279, (2006) 175-178.
[5] Maillard M., Giorgo S., Pileni M.P. *Adv.Mater.* (2002) 14(15), 1084-1086.
[6] Pillai Z.S., Kamat P.V. *J.Phys.Chem.B.* (2004) 108, 945-951.
[7] Patel K., Kapoor S., Dave D.P., Murherjee T. *J.Chem.Sci.* (2005), 117(1), 53-60.
[8] Salkar R.A., Jeevanandam P., Aruna S.T., Koltypin Y., Gedanken A. *J.Mater.Chem.* 9, (1999) 1333-1335.
[9] [9] Soroushian B., Lampre I., Belloni J., Mostafavi M. *Radiation Physics and Chemistry* (2005) 72, 111-118.
[10] Ershov B.G., Janata E., Henglein A. Fojtlk A. (2007) unpubliseh report.
[11] Starowicz M., Stypula B., Banaœ J. *Electrochemistry Communications* (2006) 8, 227-230. 2006.
[12] Zhu J.J., Liao X.H., Zhao X.N., Hen H.Y. *Materials Letters* (2001) 49, 91-95. 2001.
[13] Liu S., Chen S., Avivi S., Gendanken A., *Journal of Non-crystalline Solids* (2001) 283, 231-236.
[14] Shahverdi A.R., Fakhimi A., Shahverdi H.R., Minaian M.S. *Nonomedicine* (2007) 3, 168-171.
[15] Pal S., Kyung Y., Myong Song J. *Applied and Environmental Microbiology* (2007) 73(6), 1712-1720.
[16] Panacek,A., Kvitek L., Prucek R., Kolar M., Vecerova R., Pizurova N., Sharma V.K., Nevecna T., Zboril R. *J.Phys.Chem.B.* (2006) 110, 16248-16253.
[17] Roldán M.V., Frattini A.L., Sanctis O.A., Pellegrini N.S. *Anales AFA* 17 (2005), 212-217.
[18] Yin H., Yamamoto T., Wada Y., Yanagida S. *Materials Chemistry and Physics* 83 (2004) 66-70.
[19] Zhu Z., Kai L., Wang Y. *Materials Chemistry and Physics* 96 (2006) 447-453.
[20] A.S. Edelstein, R.C. Cammarata (Eds.) Nanomaterials, synthesis, properties and applications (1996), Bristol and Philadelphia Publishers, Bristol,
[21] Mock J.J., Barbic M., Smith D.R., Schultz D.A., Schultz S. *J.Chem.Phys.* (2002) 16(15), 6755-6759.
[22] Duran N., Marcato P.L., Alves O.L., De Souza G.I., *J.Nanobiotechnology* (2005) 3(8), 1-7.
[23] Pacios R., Marcilla R., Pozo-Gonzalo C., Pomposo J.A., Grande H., Aizpurua J., Mecerreyes D. *J.Nanosci.Nanotechnology* (2007) 7, 2938-2941.
[24] Chou,W.L., Yu,D.G., Yang,M.C. *Polym.AdV.Technol.* (2005) 16:600-608.
[25] Z. Tang, S. Liu, S. Dong, E. Wang, *Journal of Electroanalytical Chemistry* (2001) 502 ,146.
[26] M. Mazur, *Electrochemistry Communications* (2004) 6 400.
[27] Zhu Jian, Zhu Xiang, Wang Yongchang, *Mictoelectronic Engineering* 77 (2005) 58.
[28] Y.H. Kim, D.K. Lee, Y.S. Kang, *Colloids and Surfaces* A: *Physicochemical and Engineering Aspects* 257–258 (2005) 273.
[29] C.H. Bae, S.H. Nam, S.M. Park, *Applied Surface Science* 197–198, (2002) 628.
[30] Patel K., Kapoor S., Dave D.P., Ukherjee T. *J.Chem.Sci.* (2007) 117(4), 311-315.
[31] J. Zhang, P. Chen, C. Sun, X. Hu, *Applied Catalysis A:* 266, (2004) 49.

[32] Chaudhari V.R., Haram S.K., Kulshreshtha S.K. *Colloids and Surfaces A* 301 (2007) 475-480.

[33] Pal A., Shah S., Devi S. *Colloids and Surfaces* A 302 (2007), 51-57.

[34] Chen Z., Gao L. *Materials Research Bulletin* 42 (2007), 1657-1661.

[35] Kumar A., Joshi H., Pasricha R., Mandale A.B., Sastry M., *Journal of Colloid and Interface Science* 264 (2003) 396.

[36] Li D.G., Chen S.H., Zhao S.Y., Hou X.M., Ma H.Y., Yang X.G., *Thin Solid Films* 460 (2004) 78.

[37] Wang G., Shi Ch., Zhao N., Du X. *Materials Letters* 61 (2007), 3795-3797.

[38] Wilson R., Lynn G., Milosavljevic B., Meisel D. (2007) unpublished repport.

[39] Lawrence W., Barry A.L., O'toole R., Sherris J. *Applied Microbiology* 24(2) (1972), 240-247.

[40] NCCLS. 2003. Performance standards for antimicrobial susceptibility testing.Twelfth informational supplement. Rep. No. NCCLS document M100-S12. Pennsylvania.